HHS Public Access

Author manuscript

Behav Brain Res. Author manuscript; available in PMC 2018 March 30.

Published in final edited form as:

Behav Brain Res. 2017 March 30; 322(Pt B): 233–240. doi:10.1016/j.bbr.2016.09.001.

Ex vivo MRI transverse relaxation in community based older persons with and without Alzheimer's dementia

Lei Yu[1,2], **Robert J. Dawe**[1,3], **Aron S. Buchman**[1,2], **Patricia A. Boyle**[1,4], **Julie A. Schneider**[1,2,5], **Konstantinos Arfanakis**[1,6], and **David A. Bennett**[1,2]

[1]Rush Alzheimer's Disease Center, Rush University Medical Center, Chicago, IL, USA

[2]Department of Neurological Sciences, Rush University Medical Center, Chicago, IL, USA

[3]Department of Diagnostic Radiology and Nuclear Medicine, Rush University Medical Center, Chicago, IL, USA

[4]Department of Behavioral Sciences, Rush University Medical Center, Chicago, IL, USA

[5]Department of Pathology, Rush University Medical Center, Chicago, IL, USA

[6]Department of Biomedical Engineering, Illinois Institute of Technology, Chicago, IL, USA

Abstract

Alterations of the transverse relaxation rate, R_2, measured using MRI, are observed in older persons with Alzheimer's (AD) dementia. However, the spatial pattern of these alterations and the degree to which they reflect the accumulation of common age-related neuropathologies are unknown. In this study, we characterized the profile of R_2 alterations in post-mortem brains of persons with clinical diagnosis of AD dementia and investigated how the profile differs after accounting for neuropathologic indices of AD, cerebral infarcts, Lewy body disease, hippocampal sclerosis and transactive response DNA-binding protein 43. Data came from 567 post-mortem brains donated by participants in two cohort studies of aging and dementia. R_2 was quantified using fast spin echo imaging. Voxelwise linear regression examined R_2 alterations between subjects diagnosed with AD dementia at death and those with no cognitive impairment. Voxels showing significant R_2 alterations were clustered into regions of interest (ROIs). Three R_2 profiles were compared, which were adjusted for (1) demographics only; (2) demographics and AD pathology; (3) demographics, AD pathology and other common neuropathologies. R_2 alterations were observed throughout the hemisphere, most commonly in white matter. Of the distinct ROIs identified, the largest region encompassed large portions of white matter in all lobes. This ROI became smaller in size but remained largely intact after adjusting for AD and other neuropathologic indices. Further, R_2 alterations identify AD dementia with improved accuracy,

Corresponding author: David A. Bennett MD, Rush Alzheimer's Disease Center, 600 S Paulina Street, Chicago, IL 60612, David_A_Bennett@Rush.edu, Phone: 312-942-3350, Fax: 312-563-4604.

DISCLOSURE

The authors declare no conflicts of interest.

above and beyond demographics and neuropathologic indices ($p<0.0001$). In conclusion, R_2 alterations in AD dementia are not solely reflective of common age-related neuropathologies, suggesting that other mechanisms are at work.

Keywords

Ex vivo MRI; Transverse relaxation alterations; AD dementia; Age-related neuropathology

INTRODUCTION

The pathologies of Alzheimer's (AD), cerebrovascular (CVD), Lewy body diseases (LBD), hippocampal sclerosis, and the more recently discovered transactive response DNA-binding protein 43 (TDP-43) are among the most common causes of dementia in old age. The accumulation of these pathologies leads to disruption of iron homeostasis (Peters, et al., 2015) and increased free water content due to demyelination and atrophy (Zhan, et al., 2015). These changes in brain tissue properties can be detected by using magnetic resonance imaging (MRI) relaxometry, both *in vivo* and *ex vivo*. The transverse relaxation rate constant, R_2, is one such parameter which measures the decay of transverse magnetization.

Alterations of the transverse relaxation have been observed *in vivo* in older persons with memory complaints (House, et al., 2006), mild cognitive impairment, and dementia due to Alzheimer's disease (Arfanakis, et al., 2007, Bartzokis, et al., 2003, Granziera, et al., 2015, Luo, et al., 2013). Using data from *ex vivo* imaging, we previously showed that prolonged transverse relaxation time is correlated with pathologic burdens of AD, infarcts and hippocampal sclerosis, thus providing direct evidence for the neuropathologies' involvement in these alterations (Dawe, et al., 2014). Further, we demonstrated that common neuropathologic indices are not solely responsible for the relationship between transverse relaxation alterations and late life cognitive performance (Dawe, et al., 2014, Dawe, et al., 2016).

In this study, we further characterized the profile of transverse relaxation alterations in post-mortem brains of persons with AD dementia, and investigated how the profile differs after accounting for neuropathologic indices of AD, cerebral infarcts, LBD, hippocampal sclerosis and TDP-43. Data came from 567 autopsied participants in two cohort studies of aging and dementia. Transverse relaxation rate (R_2) was quantified using fast spin echo imaging. At each voxel, R_2 alteration was captured as the model adjusted difference between participants with AD dementia and those with no cognitive impairment. Significant voxels were identified and clustered into regions of interest (ROIs). Spatial distributions of ROIs were described, and comparisons were made between the profiles before and after accounting for the neuropathologies.

This current study extends our previous work (Dawe, et al., 2014, Dawe, et al., 2016) in three important ways. First, we focus on a complementary clinical outcome, i.e. diagnosis of AD dementia. While continuous cognitive measures are well-established indicators for capturing progression of AD dementia, translation of findings using cognition to the clinical context is not always straightforward. Direct comparisons of persons with AD dementia and

those with no cognitive impairment are useful in this regard and are more accessible to clinician-scientists. Second, we incorporate pathologic indices that were not included in the previous study, which provides a more thorough coverage of neuropathologic burden in older age. Third, we include additional data that are newly available and the increase in sample size provides further precision in profiling R_2 alterations.

METHODS

Study Participants

Clinical, neuropathologic, and *ex vivo* imaging data came from 567 autopsied participants in two ongoing cohort studies of aging and dementia, the Religious Orders Study (ROS) and the Rush Memory and Aging Project (MAP). Study details are described elsewhere (Bennett, et al., 2012a, Bennett, et al., 2012b). Briefly, participants were community-based older persons without known dementia at enrollment, and all agreed to annual clinical and neuropsychological evaluations and brain donation after death. Both studies were approved by the Institutional Review Board of Rush University Medical Center. Informed consent and an anatomical gift act were obtained from each participant.

By July 1st, 2016, 1,572 of the total 3,226 enrolled participants had died, and 1,358 had gone through autopsy (autopsy rate > 86%). Of the autopsied cases, 1,325 were reviewed and approved by a board certified neuropathologist. The *ex vivo* imaging project started in 2006 and is currently ongoing. At the time of analyses, there were 587 autopsied participants with processed *ex vivo* imaging data, and we excluded 20 with non-AD dementia. Of the remaining 567, 244 (43.0%) were diagnosed with AD dementia at the time of death, 153 (27.0%) with mild cognitive impairment (MCI) and 170 (30.0%) with no cognitive impairment. Primary analyses were based on those who were either diagnosed with AD dementia or no impairment (N=414). In secondary analyses, we explored R_2 alterations in participants with MCI.

Clinical diagnosis of AD dementia

Each year, participants had a uniform structured evaluation that included a physical examination and detailed cognitive testing which assessed multiple domains of cognitive abilities. Results of cognitive testing were reviewed by a neuropsychologist for the presence of cognitive impairment. Annual clinical diagnoses were made based on the evaluations by the clinician. The diagnosis of AD dementia follows the recommendation of the joint working group of the National Institute of Neurological and Communicative Disorders and Stroke and the Alzheimer's Disease and Related Disorders Association (McKhann, et al., 1984). The criteria require a history of cognitive decline and evidence of impairment in memory and at least one other cognitive domain. The criteria do not require functional impairment. We defined MCI as a derivative of the McKhann criteria but only required impairment in a single cognitive domain. MCI here is intended to identify everyone who is not cognitively normal and without dementia. Thus, all participants would be classified as having dementia (and its cause), MCI, or neither ("No cognitive impairment"). Detailed description of the implementation of the criteria is described elsewhere (Bennett, et al., 2006a, Bennett, et al., 2002).

After a participant died, a neurologist reviewed all available clinical data and provided a summary diagnostic opinion regarding the most plausible diagnosis at the time of death. The summary diagnosis was made blinded to all postmortem data, and case conferences were held for consensus on select cases, as previously described (Schneider, et al., 2007).

Ex vivo imaging and R_2 quantification

Brains were removed and bisected after death following a standard procedure (Bennett, et al., 2006b). Hemispheres chosen for imaging were fixed in 4% paraformaldehyde and stored in 4-degree Celsius refrigerators. *Ex vivo* image processing and R_2 quantification follow the same protocols as previously described (Dawe, et al., 2014, Dawe, et al., 2016). Briefly, MRI scans were performed on average 41.4 days (SD 19.8, range 23–235 days) postmortem, and each scan included a 2D turbo spin echo (TSE) sequence with multiple echo times. The R_2 value was quantified voxel by voxel from the TSE data by fitting a monoexponential decay function, and these images were spatially warped to a common template to facilitate voxelwise analyses. Because four different MRI scanners were used to acquire TSE data over the course of several years, we needed to account for instrument differences. Therefore, within each group of hemispheres imaged on a given scanner, we computed the mean and standard deviation for each voxel and used these to carry out a scanner-specific, voxel-by-voxel normalization of the R_2 values for each hemisphere.

Neuropathologic Assessments

Neuropathologic evaluations were conducted by examiners blinded to all clinical data. Hemispheres were cut coronally using a Plexiglas jig into 1-cm slabs, tissue blocks from predetermined brain regions were dissected, and 6 μm sections were stained for pathology quantification (Schneider, et al., 2012). Neuritic plaques, diffuse plaques and neurofibrillary tangles in five cortical regions were visualized using modified Bielschowsky silver stain. For each index, the counts were first scaled within region and then averaged across regions. A composite continuous measure of AD pathology was acquired by averaging summary scores of the three AD indices (Bennett, et al., 2003). Pathologic AD diagnosis according to NIA-Reagan criteria (intermediate or high likelihood) was used for descriptive purpose (Hyman and Trojanowski, 1997). Gross infarcts were identified by examining slabs and pictures from both hemispheres and confirmed histologically, as previously described (Schneider, et al., 2003). Microinfarcts were identified using hematoxylin and eosin (H&E) stain in a minimum of nine regions, including six cortical regions, two subcortical regions, and midbrain (Arvanitakis, et al., 2011). Presence of Lewy body pathology was assessed using antibodies to α-synuclein in 6 regions including substantia nigra, limbic and neocortices (Schneider, et al., 2006). Hippocampal sclerosis was identified as severe neuronal loss and gliosis in hippocampus or subiculum using H&E stain (Nag, et al., 2015). Counts of TDP43 cytoplasmic inclusions were assessed using antibodies to phosphorylated TDP-43 (pS409/410; 1:100) and a semi-quantitative measure was used to capture the staging of TDP-43 pathology from amygdala, through hippocampus or entorhinal cortex, to neocortical regions (Yu, et al., 2015).

Statistical Analysis

Demographic and neuropathologic characteristics were compared between participants with AD dementia and no cognitive impairment using *t* test, χ^2 test, or non-parametric Wilcoxon rank-sum test, as appropriate. R_2 alteration at each of the 400,000 tissue-containing voxels was examined using multivariable linear regression models. In these models, the R_2 values were the continuous outcome, and a binary indicator for diagnosis of AD dementia was the predictor. The regression coefficients estimate differences in voxelwise R_2 values between the two groups. To control for inflation of Type-I error due to multiple testing, *p*-values were adjusted using a false discovery rate (FDR) of 5%. Voxels showing significant R_2 alterations were clustered into regions of interest (ROIs), and only those regions with at least 100 contiguous voxels were retained.

The voxelwise regression analyses were repeated three times, and each time the model was controlled for additional covariates. Specifically, model 1 controlled only for demographics; model 2 controlled for demographics and AD pathology; and model 3 controlled for demographics, AD and other common pathologies. As a result, three profiles of R_2 alteration were obtained and visually compared. If R_2 alterations are largely driven by AD or other common age-related pathologies, we expect to see substantial shrinkage in size or even disappearance of ROIs from model 1 through model 3. For each significant ROI identified in the analyses in models 1 through 3, we extracted each specimen's mean normalized R_2 by averaging over all voxels within the ROI.

To investigate the contribution of R_2 in identifying AD dementia, we fit a series of logistic regression models with AD dementia versus no cognitive impairment as the binary outcome. Wald tests compared areas under the receiver operating characteristic (ROC) curve from models with and without R_2. The area under the curve, ranging from 0.5 (no discrimination) to a theoretical maximum of 1 (perfect discrimination), summarizes how accurately AD dementia was identified by each model in terms of sensitivity and specificity, and thus captures the independent contribution due to R_2.

RESULTS

Demographic and neuropathologic characteristics

Compared with participants with no cognitive impairment, participants with AD dementia were older (Table 1). We did not observe significant difference in sex, race, or years of education between the two groups. Consistent with our previous report (Bennett, et al., 2012c), age-related pathologies were common in post-mortem brains of participants with no cognitive impairment. Notably, almost half (48.2%) of those participants met NIA-Reagan criteria for pathologic AD, 31.8% had gross infarcts, and 18.8% had Lewy bodies. On the other hand, participants with AD dementia on average had more severe AD and TDP-43 pathologies, and were more likely to have gross infarcts, Lewy bodies, and hippocampal sclerosis (Table 1). Comorbidities were also much more common in AD dementia. Almost 90% of the subjects with AD dementia had multiple neuropathologies present in their brains, in comparison with 54.7% of those with no cognitive impairment.

R_2 alterations in AD dementia

We first examined the R_2 alterations in AD dementia without adjusting for any neuropathology (model 1). R_2 alterations were widespread across the whole hemisphere, and most commonly observed in white matter (Figure 1-A). Two separate regions were identified. For each region, the location, volume, and the average difference in the R_2 value are summarized in Table 2. Briefly, the largest region (region 1) of R_2 alterations covered large portions of the white matter in the frontal lobe, and extended to the white matter in the parietal, occipital and temporal lobes. The transverse relaxation rate in this region was on average slower in AD dementia, compared with no cognitive impairment. The second region was in the insular gray matter and had much smaller volume. Notably, the transverse relaxation rate in this gray matter region was faster in AD dementia.

Since AD pathology is the primary driver of dementia and prior work suggests it is strongly associated with R_2 alterations, we refit the model by controlling for demographics and the overall burden of AD pathology (model 2). Three separate regions were identified, and we observed a certain amount of shrinkage in the size of regions showing R_2 alterations (Figure 1-B). The largest region involved the white matter of all four lobes. This and a smaller region in white matter of the parietal lobe were derivatives of region 1 from the previous model, and transverse relaxation rates in both regions were slower in AD dementia. The third region was in the insular gray matter, with faster transverse relaxation rate in AD dementia (Table 2).

Next, we augmented the model by controlling for cerebral infarcts, Lewy body, hippocampal sclerosis, and TDP-43 pathologies in addition to demographics and AD pathology (model 3). In this model, we observed further shrinkage in size of regions showing significant R_2 alterations (Figure 1-C). Nonetheless, substantial R_2 alterations remained. Of the five regions identified, four were derivatives of region 1 from the first model. While split and smaller in size, they still encompassed large portions of the frontal, parietal, occipital and temporal lobe white matter. Consistent with the results from the previous models, the transverse relaxation rates in these white matter regions were slower in AD dementia. By contrast, the fifth region observed in the insular gray matter again showed faster transverse relaxation rate in AD dementia (Table 2). Figure 2 provides three-dimensional contrast of the R_2 alterations in AD demenita from all three models. Regions in green are derived from model 1 which controlled for demographics only, regions in blue are from model 2 which controlled for demographics and AD pathology, and regions in purple are from model 3 which controlled for demographics, AD pathology and other neuropathologies.

R_2 contributes to the risk of AD dementia

The persistent presence of R_2 alterations in postmortem brain of participants with AD dementia suggests that not all the R_2 alterations are reflective of neuropathologies measured in this study. In the final set of analyses, we investigated whether R_2 holds utility in identifying subjects with AD dementia compared to those with no cognitive impairment. We focused on the R_2 values in the five regions acquired from the last model (model 3). Comparisons of areas under the ROC curve show that R_2 in these 5 regions improved the accuracy of identifying AD dementia (Figure 3). Specifically, the area under the curve from

the model adjusted for demographics and AD pathology was 0.75, and inclusion of other pathologic indices increased the area to 0.82 (p=0.0001). By including the measure of R_2 alterations, the area under the curve was further increased to 0.88 (p<0.0001).

R_2 alterations in mild cognitive impairment

Finally, we repeated the voxel-wise regression analyses to examine R_2 alterations in cases of MCI. The initial voxelwise analysis of all ~400,000 tissue-containing voxels did not yield any significant region that satisfied both the 5% FDR for voxels and the minimum size requirement (i.e. 100 contiguous voxels) for regions. To reduce the burden of multiple testing, in a *post hoc* exploratory analysis, we constrained the analysis to voxels showing significant R_2 alterations in model 3 for AD dementia. We identified 4 separate regions with evidence of slower transverse relaxation rate in MCI, which were scattered in white matter of the frontal, and parietal or occipital lobes (Supplemental Figure 1). Inclusion of the R_2 measures from these regions increased the area under the ROC curve for identifying MCI from 0.63 to 0.68, yet it didn't reach the common threshold for statistical significance (p=0.052).

DISCUSSION

In this study, we leveraged clinical, neuropathologic and *ex vivo* imaging data from hundreds of community-based older persons to examine the profiles of voxelwise R_2 alterations in AD dementia. Our findings suggest that R_2 alterations span the entire hemisphere, including large portions of white matter. We observed an overall reduction in volume of significant R_2 alterations after accounting for AD pathology and other neuropathologic indices that are known to cause dementia. However, R_2 alterations remained prominent across all four lobes. We further demonstrated that R_2 alterations identify AD dementia with improved accuracy, above and beyond demographics and neuropathologic indices. To our knowledge, no prior study has examined the degree to which R_2 alterations in AD dementia are reflective of the accumulation of common age-related neuropathologies.

We observed *ex vivo* white matter R_2 alterations in AD dementia. The main regions are found in the white matter with significant reduction of R_2. This finding is consistent with prior findings, both *in vivo* and *ex vivo*. An earlier study estimates that frontal white matter R_2 in AD patients is 1 standard deviation below that of controls (Bartzokis, et al., 2003). A more recent study extends the finding by showing that reduction of R_2 is also present in other white matter regions including temporal lobe and internal capsule (House, et al., 2006). It has also been reported that *ex vivo* transverse relaxation is slower in parietal and temporal white matter of pathologically confirmed Alzheimer's (Besson, et al., 1992).

We compared the profiles of R_2 alterations before and after accounting for AD pathology and other neuropathologic indices. Our findings have several implications. First, the results lend further support that age-related pathologies known to cause dementia contribute to white matter damage in AD dementia. Regions showing R_2 alterations became smaller in size after we adjusted the model by controlling for AD pathology. Biochemical analyses of AD white matter also confirm that extensive axonal demyelination underlies Alzheimer's pathology (Roher, et al., 2002). Other evidence, however, suggests that morphological

components such as astrocyte to oligodendrocyte ratio differ between white matter disease and Alzheimer's disease (Sjobeck and Englund, 2003). Indeed, while AD pathology is the main driver of dementia, the presence of R_2 alterations remains evident after adjusting for the measure of AD pathology. Mounting evidence from histopathological studies demonstrates that AD pathology is often accompanied by other comorbid conditions and mixed pathologies are the most common cause of dementia (Barnes, et al., 2015, James, et al., 2012, Schneider, et al., 2009, White, et al., 2016). This is true in the current study in which almost 90% of the cases with AD dementia exhibited multiple neuropathologies. After accounting for cerebral infarcts, Lewy bodies, hippocampal sclerosis and TDP-43 pathologies, we observe further shrinkage of the regions with R_2 alterations.

The persistence of R_2 alterations in a large area of white matter after adjustment for common age-related neuropathologies suggests that white matter change is not solely reflective of commonly measured neuropathologies. Investigation of other mechanisms that underlie R_2 alterations may provide novel therapeutic targets to combat late life cognitive impairment and dementia. One potential contributor is vascular burden, which may in part be reflected by white matter hyperintensities (WMHs). Increase in WMHs in prefrontal cortex is associated with age-related changes in memory functioning (Nordahl, et al., 2006). Recent studies indicate that WMHs have little impact on the progression of Alzheimer's specific biomarkers (Lo and Jagust, 2012) and affect late life cognitive decline independent of amyloid pathology (Vemuri, et al., 2015). Progression of WMHs in the parietal lobe, but not other regions, may predict incident AD dementia (Brickman, et al., 2015). Future studies need to disentangle the relationship of WMHs and R_2 alterations in AD dementia. Notably, our *ex vivo* data show that R_2 alterations improve the accuracy of identifying AD dementia, in addition to the common neuropathologic indices. We have previously demonstrated a linear relationship between *in vivo* and *ex vivo* R_2 measures (Dawe, et al., 2014). Taken together, our results suggest that *in vivo* R_2 alterations may serve as a biomarker for AD dementia, in addition to other markers such as PIB-PET (Pittsburgh compound B PET).

We only captured very limited R_2 alterations in gray matter. We identified one region in the insular gray matter where R_2 is greater in AD dementia. A related finding in the same cohort has been reported previously, where T_2 (reciprocal of R_2) shortening in the insula is associated with more AD pathology (Dawe, et al., 2014). This relationship may be attributable to elevated redox-active iron concentration, in part as the consequence of plaque and tangle accumulations (Smith, et al., 1997). However, new data from this study further demonstrate that the insular R_2 alterations are not fully explained by AD pathology or several other common age-related pathologies. This new finding renders support that other factors may contribute to the disruption of iron homeostasis in AD dementia. One plausible explanation for lack of R_2 alterations in gray matter was noted previously in hippocampus (Schenck, et al., 2006). The transverse relaxation rate accelerates with increasing iron concentration but decelerates with increasing water content. Both effects may occur and offset each other, more likely so in gray matter. Studies show that, with increasing age, brain ferritin iron level is elevated in cortical and subcortical gray matter, but lower in frontal white matter (Bartzokis, et al., 2007). Higher iron concentration induces oxidative damage (Quintana, et al., 2006, Smith, et al., 1997) and leads to myelin breakdown (Bartzokis,

2011). This demyelination, in turn, contributes to increasing free water content in brain tissue, which has a slowing effect on R_2.

The overall findings in this study are consistent with our prior work on late life cognitive function (Dawe, et al., 2014, Dawe, et al., 2016). Both suggest that R_2 alterations are implicated in cognition and AD dementia, above and beyond the influences of common age-related brain pathologies. This work expands upon our previous findings in several important ways. First, we elected to use a complementary clinical outcome of AD dementia, and findings from the current work provide information specific to disease status (i.e. AD dementia versus no impairment), a comparison that cannot be easily achieved via continuous cognitive measures. We are not aware of any study that has directly profiled the spatial patterns of transverse relaxation alterations in community based older persons with AD dementia relative to persons with no cognitive impairment. Second, we incorporated additional pathologic indices that were not previously investigated, which provides a more thorough coverage of neuropathologic burden in older age. Specifically, we included indices for Lewy body pathology and a less well-studied pathology, transactive response DNA-binding protein 43 (TDP-43). Recent studies suggest that these pathologies are quite common among older persons and their inclusion expands on our prior work and helps calibrate the profile of R_2 alterations in AD dementia. Third, the present findings contribute to the growing body of literature suggesting that AD dementia reflects multiple disease processes. AD dementia was long thought to be due to a single disease specific to plaques and tangles. By directly interrogating the profile of R_2 between subjects with and without AD dementia, before and after adjusting for contributions of AD and other non-AD pathologies, we provide novel evidence which identify other mechanism that contributes to AD dementia. This cannot be readily deduced from our prior work.

The study has strength and limitations. Data came from two studies of aging that require annual clinical evaluations and brain donation after death to support the collection of neuropathology and *ex vivo* imaging data. This study design allows us to efficiently merge different data from the same participants and examine the correlates of clinical and imaging features above and beyond the influence of neuropathology. The voxelwise approach of identifying R_2 alterations provides comprehensive coverage throughout the entire brain hemisphere. Limitations include the use of only one modality, namely R_2. *Ex vivo* imaging is not capable of capturing longitudinal change in R_2. Finally, participants in the study are older and have higher education, and our findings may not be generalizable to the general population.

Supplementary Material

Refer to Web version on PubMed Central for supplementary material.

Acknowledgments

FUNDING

This research was supported by NIA grants R01AG17917, P30AG10161, R01AG34374, and the Illinois Department of Public Health.

The authors thank the participants of the Religious Orders Study and the Rush Memory and Aging Project for their invaluable contributions. We also thank all the investigators and the staff of the Rush Alzheimer's Disease Center.

References

Arfanakis K, Gui M, Tamhane AA, Carew JD. Investigating the Medial Temporal Lobe in Alzheimer's Disease and Mild Cognitive Impairment, with Turboprop Diffusion Tensor Imaging, MRI-volumetry, and T 2-relaxometry. Brain Imaging and Behavior. 2007; 1(1):11–21. DOI: 10.1007/s11682-007-9001-4

Arvanitakis Z, Leurgans SE, Barnes LL, Bennett DA, Schneider JA. Microinfarct pathology, dementia, and cognitive systems. Stroke; a journal of cerebral circulation. 2011; 42(3):722–7. DOI: 10.1161/strokeaha.110.595082

Barnes LL, Leurgans S, Aggarwal NT, Shah RC, Arvanitakis Z, James BD, Buchman AS, Bennett DA, Schneider JA. Mixed pathology is more likely in black than white decedents with Alzheimer dementia. Neurology. 2015; 85(6):528–34. DOI: 10.1212/wnl.0000000000001834 [PubMed: 26180136]

Bartzokis G. Alzheimer's disease as homeostatic responses to age-related myelin breakdown. Neurobiology of aging. 2011; 32(8):1341–71. DOI: 10.1016/j.neurobiolaging.2009.08.007 [PubMed: 19775776]

Bartzokis G, Cummings JL, Sultzer D, Henderson VW, Nuechterlein KH, Mintz J. White matter structural integrity in healthy aging adults and patients with Alzheimer disease: a magnetic resonance imaging study. Arch Neurol. 2003; 60(3):393–8. [PubMed: 12633151]

Bartzokis G, Tishler TA, Lu PH, Villablanca P, Altshuler LL, Carter M, Huang D, Edwards N, Mintz J. Brain ferritin iron may influence age- and gender-related risks of neurodegeneration. Neurobiology of aging. 2007; 28(3):414–23. DOI: 10.1016/j.neurobiolaging.2006.02.005 [PubMed: 16563566]

Bennett DA, Schneider JA, Aggarwal NT, Arvanitakis Z, Shah RC, Kelly JF, Fox JH, Cochran EJ, Arends D, Treinkman AD, Wilson RS. Decision rules guiding the clinical diagnosis of Alzheimer's disease in two community-based cohort studies compared to standard practice in a clinic-based cohort study. Neuroepidemiology. 2006a; 27(3):169–76. DOI: 10.1159/000096129 [PubMed: 17035694]

Bennett DA, Schneider JA, Arvanitakis Z, Kelly JF, Aggarwal NT, Shah RC, Wilson RS. Neuropathology of older persons without cognitive impairment from two community-based studies. Neurology. 2006b; 66(12):1837–44. DOI: 10.1212/01.wnl.0000219668.47116.e6 [PubMed: 16801647]

Bennett DA, Schneider JA, Arvanitakis Z, Wilson RS. Overview and findings from the Religious Orders Study. Current Alzheimer research. 2012a; 9(6):628–45. [PubMed: 22471860]

Bennett DA, Schneider JA, Buchman AS, Barnes LL, Boyle PA, Wilson RS. Overview and findings from the Rush Memory and Aging Project. Current Alzheimer research. 2012b; 9(6):646–63. [PubMed: 22471867]

Bennett DA, Wilson RS, Boyle PA, Buchman AS, Schneider JA. Relation of neuropathology to cognition in persons without cognitive impairment. Annals of neurology. 2012c; 72(4):599–609. [PubMed: 23109154]

Bennett DA, Wilson RS, Schneider JA, Evans DA, Aggarwal NT, Arnold SE, Cochran EJ, Berry-Kravis E, Bienias JL. Apolipoprotein E epsilon4 allele, AD pathology, and the clinical expression of Alzheimer's disease. Neurology. 2003; 60(2):246–52. [PubMed: 12552039]

Bennett DA, Wilson RS, Schneider JA, Evans DA, Beckett LA, Aggarwal NT, Barnes LL, Fox JH, Bach J. Natural history of mild cognitive impairment in older persons. Neurology. 2002; 59(2):198–205. [PubMed: 12136057]

Besson JA, Best PV, Skinner ER. Post-mortem proton magnetic resonance spectrometric measures of brain regions in patients with a pathological diagnosis of Alzheimer's disease and multi-infarct dementia. The British journal of psychiatry : the journal of mental science. 1992; 160:187–90. [PubMed: 1540758]

Brickman AM, Zahodne LB, Guzman VA, Narkhede A, Meier IB, Griffith EY, Provenzano FA, Schupf N, Manly JJ, Stern Y, Luchsinger JA, Mayeux R. Reconsidering harbingers of dementia: progression of parietal lobe white matter hyperintensities predicts Alzheimer's disease incidence.

Neurobiology of aging. 2015; 36(1):27–32. DOI: 10.1016/j.neurobiolaging.2014.07.019 [PubMed: 25155654]

Dawe RJ, Bennett DA, Schneider JA, Leurgans SE, Kotrotsou A, Boyle PA, Arfanakis K. Ex vivo T2 relaxation: associations with age-related neuropathology and cognition. Neurobiology of aging. 2014; 35(7):1549–61. DOI: 10.1016/j.neurobiolaging.2014.01.144 [PubMed: 24582637]

Dawe RJ, Yu L, Leurgans SE, Schneider JA, Buchman AS, Arfanakis K, Bennett DA, Boyle PA. Postmortem MRI: a novel window into the neurobiology of late life cognitive decline. Neurobiology of aging. 2016; 45:169–77. doi:http://dx.doi.org/10.1016/j.neurobiolaging.2016.05.023. [PubMed: 27459937]

Granziera C, Daducci A, Donati A, Bonnier G, Romascano D, Roche A, Bach Cuadra M, Schmitter D, Kloppel S, Meuli R, von Gunten A, Krueger G. A multi-contrast MRI study of microstructural brain damage in patients with mild cognitive impairment. NeuroImage Clinical. 2015; 8:631–9. DOI: 10.1016/j.nicl.2015.06.003 [PubMed: 26236628]

House MJ, St Pierre TG, Foster JK, Martins RN, Clarnette R. Quantitative MR imaging R2 relaxometry in elderly participants reporting memory loss. AJNR American journal of neuroradiology. 2006; 27(2):430–9. [PubMed: 16484425]

Hyman BT, Trojanowski JQ. Consensus recommendations for the postmortem diagnosis of Alzheimer disease from the National Institute on Aging and the Reagan Institute Working Group on diagnostic criteria for the neuropathological assessment of Alzheimer disease. Journal of neuropathology and experimental neurology. 1997; 56(10):1095–7. [PubMed: 9329452]

James BD, Bennett DA, Boyle PA, Leurgans S, Schneider JA. Dementia from Alzheimer disease and mixed pathologies in the oldest old. JAMA : the journal of the American Medical Association. 2012; 307(17):1798–800. DOI: 10.1001/jama.2012.3556 [PubMed: 22550192]

Lo RY, Jagust WJ. Vascular burden and Alzheimer disease pathologic progression. Neurology. 2012; 79(13):1349–55. DOI: 10.1212/WNL.0b013e31826c1b9d [PubMed: 22972646]

Luo Z, Zhuang X, Kumar D, Wu X, Yue C, Han C, Lv J. The correlation of hippocampal T2-mapping with neuropsychology test in patients with Alzheimer's disease. PloS one. 2013; 8(9):e76203.doi: 10.1371/journal.pone.0076203 [PubMed: 24098779]

McKhann G, Drachman D, Folstein M, Katzman R, Price D, Stadlan EM. Clinical diagnosis of Alzheimer's disease: report of the NINCDS-ADRDA Work Group under the auspices of Department of Health and Human Services Task Force on Alzheimer's Disease. Neurology. 1984; 34(7):939–44. [PubMed: 6610841]

Nag S, Yu L, Capuano AW, Wilson RS, Leurgans SE, Bennett DA, Schneider JA. Hippocampal sclerosis and TDP-43 pathology in aging and Alzheimer disease. Annals of neurology. 2015; 77(6):942–52. DOI: 10.1002/ana.24388 [PubMed: 25707479]

Nordahl CW, Ranganath C, Yonelinas AP, Decarli C, Fletcher E, Jagust WJ. White matter changes compromise prefrontal cortex function in healthy elderly individuals. Journal of cognitive neuroscience. 2006; 18(3):418–29. DOI: 10.1162/089892906775990552 [PubMed: 16513006]

Peters DG, Connor JR, Meadowcroft MD. The relationship between iron dyshomeostasis and amyloidogenesis in Alzheimer's disease: Two sides of the same coin. Neurobiology of disease. 2015; 81:49–65. DOI: 10.1016/j.nbd.2015.08.007 [PubMed: 26303889]

Quintana C, Bellefqih S, Laval JY, Guerquin-Kern JL, Wu TD, Avila J, Ferrer I, Arranz R, Patino C. Study of the localization of iron, ferritin, and hemosiderin in Alzheimer's disease hippocampus by analytical microscopy at the subcellular level. Journal of structural biology. 2006; 153(1):42–54. DOI: 10.1016/j.jsb.2005.11.001 [PubMed: 16364657]

Roher AE, Weiss N, Kokjohn TA, Kuo YM, Kalback W, Anthony J, Watson D, Luehrs DC, Sue L, Walker D, Emmerling M, Goux W, Beach T. Increased A beta peptides and reduced cholesterol and myelin proteins characterize white matter degeneration in Alzheimer's disease. Biochemistry. 2002; 41(37):11080–90. [PubMed: 12220172]

Schenck JF, Zimmerman EA, Li Z, Adak S, Saha A, Tandon R, Fish KM, Belden C, Gillen RW, Barba A, Henderson DL, Neil W, O'Keefe T. High-field magnetic resonance imaging of brain iron in Alzheimer disease. Topics in magnetic resonance imaging : TMRI. 2006; 17(1):41–50. DOI: 10.1097/01.rmr.0000245455.59912.40 [PubMed: 17179896]

Schneider JA, Arvanitakis Z, Bang W, Bennett DA. Mixed brain pathologies account for most dementia cases in community-dwelling older persons. Neurology. 2007; 69(24):2197–204. DOI: 10.1212/01.wnl.0000271090.28148.24 [PubMed: 17568013]

Schneider JA, Arvanitakis Z, Leurgans SE, Bennett DA. The neuropathology of probable Alzheimer disease and mild cognitive impairment. Annals of neurology. 2009; 66(2):200–8. DOI: 10.1002/ana.21706 [PubMed: 19743450]

Schneider JA, Arvanitakis Z, Yu L, Boyle PA, Leurgans SE, Bennett DA. Cognitive impairment, decline and fluctuations in older community-dwelling subjects with Lewy bodies. Brain. 2012; 135(Pt 10):3005–14. DOI: 10.1093/brain/aws234 [PubMed: 23065790]

Schneider JA, Li JL, Li Y, Wilson RS, Kordower JH, Bennett DA. Substantia nigra tangles are related to gait impairment in older persons. Annals of neurology. 2006; 59(1):166–73. DOI: 10.1002/ana.20723 [PubMed: 16374822]

Schneider JA, Wilson RS, Cochran EJ, Bienias JL, Arnold SE, Evans DA, Bennett DA. Relation of cerebral infarctions to dementia and cognitive function in older persons. Neurology. 2003; 60(7):1082–8. [PubMed: 12682310]

Sjobeck M, Englund E. Glial levels determine severity of white matter disease in Alzheimer's disease: a neuropathological study of glial changes. Neuropathol Appl Neurobiol. 2003; 29(2):159–69. [PubMed: 12662323]

Smith MA, Harris PL, Sayre LM, Perry G. Iron accumulation in Alzheimer disease is a source of redox-generated free radicals. Proc Natl Acad Sci U S A. 1997; 94(18):9866–8. [PubMed: 9275217]

Vemuri P, Lesnick TG, Przybelski SA, Knopman DS, Preboske GM, Kantarci K, Raman MR, Machulda MM, Mielke MM, Lowe VJ, Senjem ML, Gunter JL, Rocca WA, Roberts RO, Petersen RC, Jack CR Jr. Vascular and amyloid pathologies are independent predictors of cognitive decline in normal elderly. Brain. 2015; 138(Pt 3):761–71. DOI: 10.1093/brain/awu393 [PubMed: 25595145]

White LR, Edland SD, Hemmy LS, Montine KS, Zarow C, Sonnen JA, Uyehara-Lock JH, Gelber RP, Ross GW, Petrovitch H, Masaki KH, Lim KO, Launer LJ, Montine TJ. Neuropathologic comorbidity and cognitive impairment in the Nun and Honolulu-Asia Aging Studies. Neurology. 2016; 86(11):1000–8. DOI: 10.1212/wnl.0000000000002480 [PubMed: 26888993]

Yu L, De Jager PL, Yang J, Trojanowski JQ, Bennett DA, Schneider JA. The TMEM106B locus and TDP-43 pathology in older persons without FTLD. Neurology. 2015; 84(9):927–34. DOI: 10.1212/wnl.0000000000001313 [PubMed: 25653292]

Zhan X, Jickling GC, Ander BP, Stamova B, Liu D, Kao PF, Zelin MA, Jin LW, DeCarli C, Sharp FR. Myelin basic protein associates with AbetaPP, Abeta1–42, and amyloid plaques in cortex of Alzheimer's disease brain. Journal of Alzheimer's disease : JAD. 2015; 44(4):1213–29. DOI: 10.3233/jad-142013 [PubMed: 25697841]

Highlights

- *Ex vivo* R_2 alterations are pervasive in brains with AD dementia.
- R_2 alterations are smaller in size after accounting for common neuropathologies.
- R_2 alterations in white matter remain after accounting for common neuropathologies.
- R_2 alterations identify AD dementia with improved accuracy.

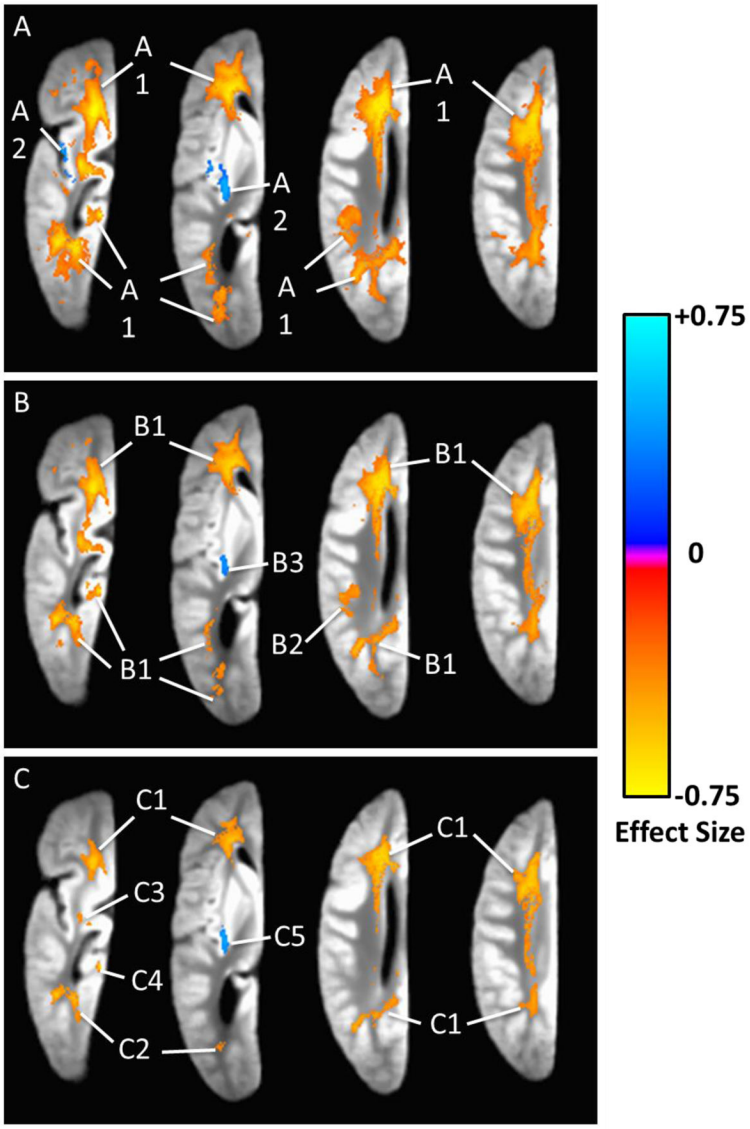

Figure 1.

Ex vivo R_2 alterations in AD dementia captured using voxelwise linear regression models. Axial views of a single hemisphere are shown, with colors indicating the magnitude and direction of the association. Figure 1-A is based on the results from models controlling for demographics only. Figure 1-B is based on the results from models controlling for demographics and AD pathology. Figure 1-C is based on the results from models controlling for demographics, AD pathology, cerebral infarcts, hippocampal sclerosis, Lewy body, and TDP-43 pathologies.

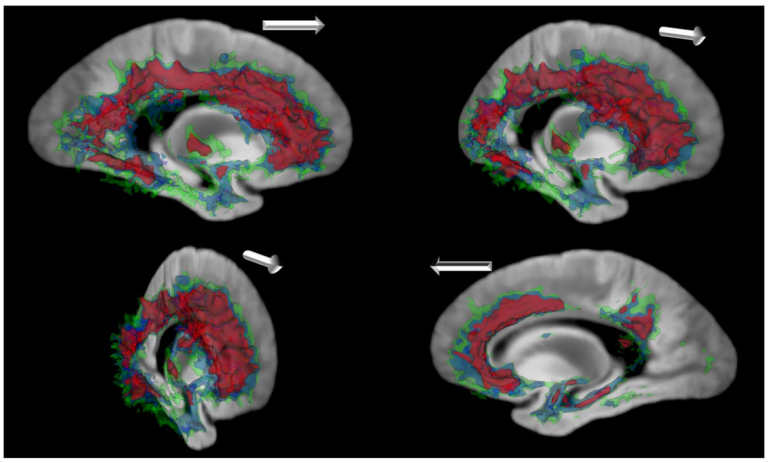

Figure 2.

Three-dimensional rendering of the R_2 alterations in AD dementia from models controlling for demographics only (green), demographics and AD pathology (blue), and demographics, AD pathology, and hippocampal sclerosis, cerebral infarcts, Lewy bodies, and TDP-43 pathologies (purple). The white arrow is oriented toward the anterior portion of the brain in each oblique-sagittal viewpoint.

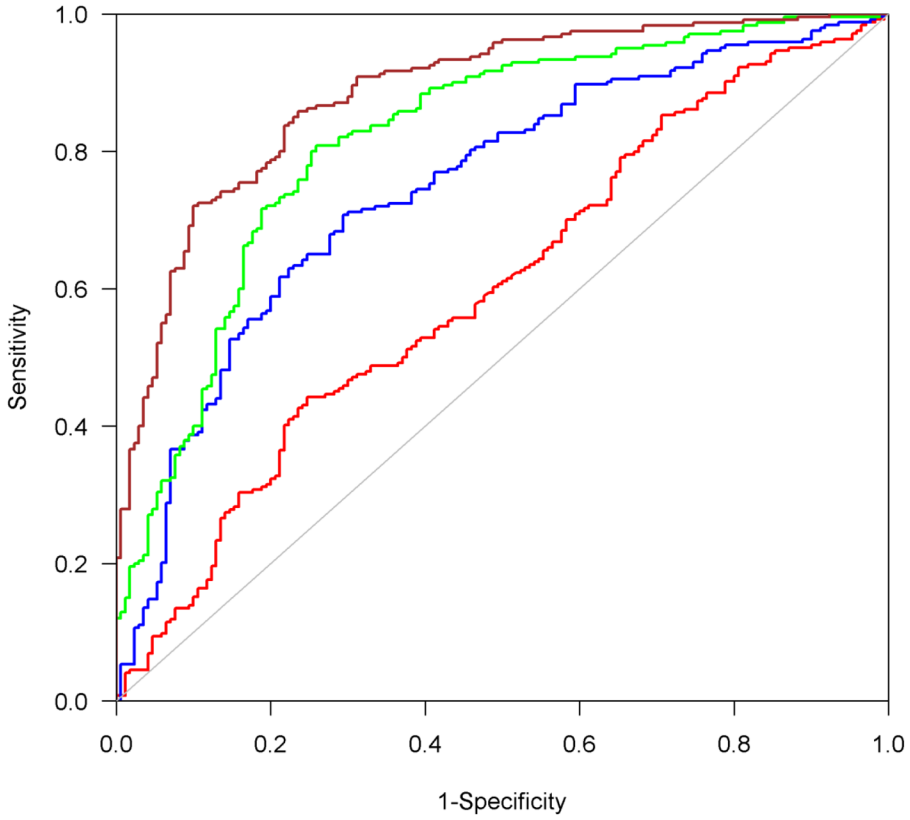

Figure 3.

The area under the ROC curves for four logistic regression models with AD dementia being the binary outcome. The area between blue and red curves is the improvement of predictive accuracy after AD pathology is added to the model with only age and sex. The area between green and blue curves is the improvement of predictive accuracy after adding 4 additional neuropathologic indices: cerebral infarcts, Lewy bodies, hippocampal sclerosis and TDP-43. The area between brown and green curves is the improvement of predictive accuracy after adding R_2.

Table 1

Demographic and neuropathologic characteristics

	AD dementia (N=244)	Mild cognitive impairment (N=153)	No cognitive impairment (N=170)	*P*
Age in years	91.0 (6.0)	90.3 (5.6)	88.9 (6.4)	<.0001
Female sex, %	73.4%	70.6%	68.8%	0.314
Non-Hispanic whites	95.9%	97.4%	95.3%	0.766
Education in years	15.7 (3.6)	15.8 (3.7)	15.9 (3.6)	0.647
PMII in days	42.3 (18.6)	39.3 (17.9)	41.9 (22.8)	0.866
AD Pathology	1.04 (0.67)	0.68 (0.55)	0.53 (0.50)	<.0001
Gross infarcts, %	49.2%	39.9%	31.8%	<.0001
Microinfarcts, %	34.8%	37.3%	36.5%	0.732
Lewy body pathology, %	31.7%	16.3%	18.8%	0.004
Hippocampal sclerosis, %	22.1%	7.2%	3.5%	<.0001
TDP-43 staging, %				
0	31.0%	46.1%	56.5%	<.0001
1	14.9%	20.4%	19.4%	
2	26.9%	21.1%	18.8%	
3	27.3%	12.5%	5.3%	

Data are presented as mean (SD) unless otherwise indicated

Group comparisons are done between AD dementia and no cognitive impairment

PMII: postmortem interval to imaging

TDP-43 staging; 0: no inclusions; 1: inclusions in amygdala only; 2: inclusions in amygdala, and entorhinal cortex or hippocampus CA1; 3: inclusions in amygdala, entorhinal cortex or hippocampus CA1, and neocortex.

Table 2

Regions with R_2 alterations in AD dementia[†]

Model #	Regions identifier	Principal location (volume, $\bar{\beta}$)
Model 1	Region 1	Large portions of WM of all lobes (volume: 57,180 mm^3, $\bar{\beta}$: −0.265)
Model 1	Region 2	Insular GM (volume: 1,126 mm^3, $\bar{\beta}$: 0.287)
Model 2	Region 1	Large portions of WM of all lobes (volume: 36,172 mm^3,$\bar{\beta}$: −0.349)
Model 2	Region 2	Parietal WM (volume: 825 mm^3, $\bar{\beta}$: −0.295)
Model 2	Region 3	Insular GM (volume: 202 mm^3, $\bar{\beta}$: 0.311)
Model 3	Region 1	Large portions of WM of all lobes (volume: 16,924 mm^3, $\bar{\beta}$: −0.366)
Model 3	Region 2	Temporal WM (volume: 1,163 mm^3, $\bar{\beta}$: −0.338)
Model 3	Region 3	Temporal WM (volume: 216 mm^3, $\bar{\beta}$: −0.306)
Model 3	Region 4	Temporal/parahippocampal WM (volume: 243 mm^3, $\bar{\beta}$: −0.325)
Model 3	Region 5	Insular GM (volume: 232 mm^3, $\bar{\beta}$: 0.348)

[†]Regions due to artifact of brain atrophy that are sensitive to outliers are not included.

Each region is described in terms of principal location, volume (mm^3), and $\bar{\beta}$ that represents the difference in standard deviation of R_2 values between AD dementia and no cognitive impairment. Model 1 is adjusted only for age and sex; model 2 is adjusted for age, sex and AD pathology; and model 3 is adjusted for age, sex, AD, cerebral infarcts, Lewy bodies, hippocampal sclerosis, and TDP-43 pathologies.

WM: white matter, GM: gray matter